Accepted Manuscript

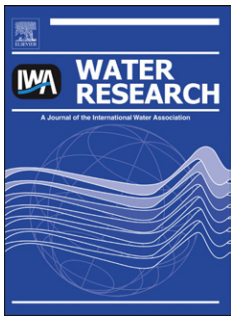

Photocatalytic degradation of endocrine disruptor compounds under simulated solar light

Vanessa Maroga Mboula, Valº rie Hº quet, Yves Andr¹ s, Luisa Maria Pastrana-Mart³ínez, Josº Miguel DoÂa-Rodr³íguez, Adri² n M.T. Silva, Polycarpos Falaras

PII: S0043-1354(13)00192-9

DOI: 10.1016/j.watres.2013.01.055

Reference: WR 9823

To appear in: *Water Research*

Received Date: 31 May 2012

Revised Date: 21 December 2012

Accepted Date: 24 January 2013

Please cite this article as: Mboula, V.M., Hº quet, V., Andr¹ s, Y., Pastrana-Mart³ínez, L.M., DoÂa-Rodr³íguez, J.M., Silva, A.M.T., Falaras, P., Photocatalytic degradation of endocrine disruptor compounds under simulated solar light, *Water Research* (2013), doi: 10.1016/j.watres.2013.01.055.

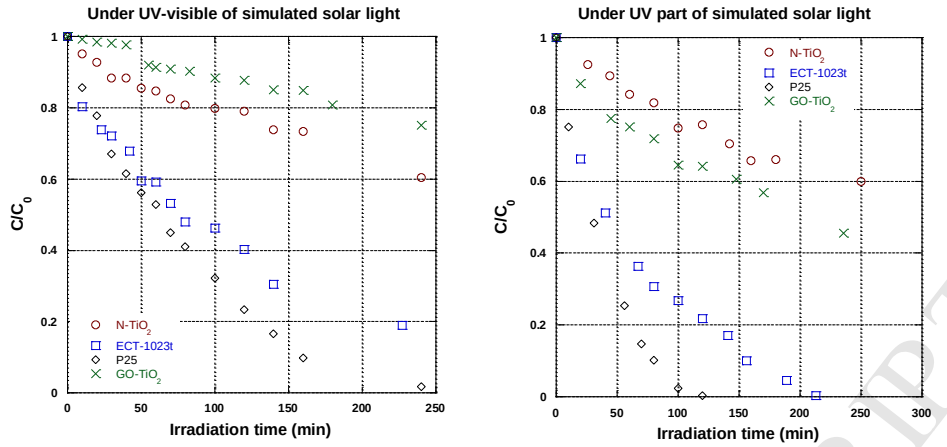

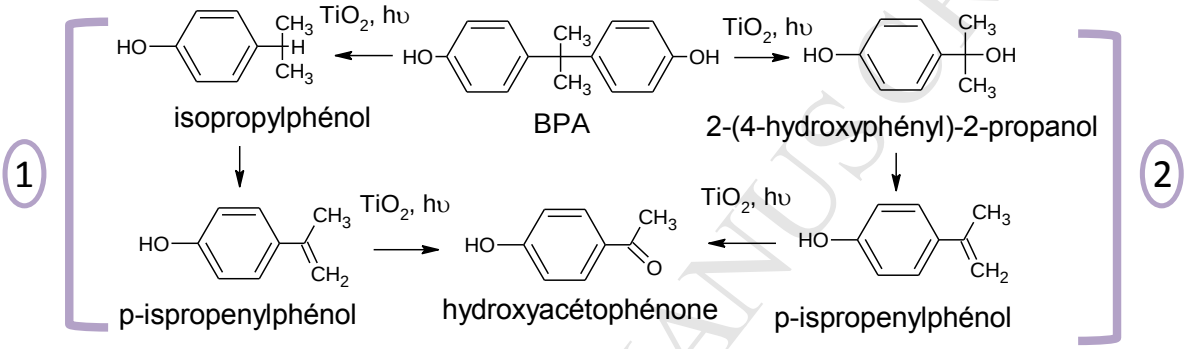

Photocatalytic reaction pathway depends on the catalysts used

Photocatalytic degradation of endocrine disruptor compounds under simulated solar light

Vanessa Maroga Mboula[a], Valérie Héquet[a], Yves Andrès[a], Luisa Maria Pastrana-Martínez[c], José Miguel Doña-Rodríguez[b], Adrián M. T. Silva[c] and Polycarpos Falaras[d]

[a] LUNAM Université, Ecole des Mines de Nantes, CNRS, GEPEA, UMR 6144, 4 rue Alfred Kastler, 44307 Nantes cedex 03, France

[b] FEAM-Departamento de Química, Universidad de Las Palmas de Gran Canaria, Edificio Central del Parque Científico-Tecnológico de la ULPGC, Campus Universitario de Tafira, 35017 Las Palmas, Spain

[c] LCM – Laboratory of Catalysis and Materials – Associate Laboratory LSRE/LCM, Faculdade de Engenharia, Universidade do Porto, Rua Dr. Roberto Frias, 4200-465 Porto, Portugal

[d] Institute of Physical Chemistry, NCSR Demokritos, 153 10 Aghia Paraskevi Attikis, Athens, Greece

Abstract

Nanostructured titanium materials with high UV-visible activity were synthesized in the collaborative project Clean Water FP7. In this study, the efficiency of some of these catalysts to degrade endocrine disruptor compounds, using bisphenol A as the model compound, was evaluated. Titanium dioxide P25 (AEROXIDE® TiO_2, Evonik Degussa) was used as the reference. The photocatalytic degradation was carried out under the UV part of a simulated solar light (280-400 nm) and under the

full spectrum of a simulated solar light (280 nm-30 µm). Catalytic efficiency was assessed using several indicators such as the conversion yield, the mineralization yield, by-product formation and the endocrine disruption effect of by-products. The new synthesized catalysts exhibited a significant degradation of bisphenol A, with the so-called ECT-1023t being the most efficient. The intermediates formed during photocatalytic degradation experiments with ECT-1023t as catalyst were monitored and identified. The estrogenic effect of the intermediates was also evaluated *in vivo* using a ChgH-GFP transgenic medaka line. The results obtained show that the formation of intermediates is related to the nature of the catalyst and depends on the experimental conditions. Moreover, under simulated UV, in contrast with the results obtained using P25, the by-products formed with ECT-1023t as catalyst do not present an estrogenic effect.

Keywords

Photocatalysis, simulated solar light, estrogenic effect, reaction pathway

1. Introduction

During recent decades, bisphenol A (BPA) has gained attention and become a public concern since it was recognized as causing an endocrine disruption effect (Staples *et al.*, 1998; Birkett and Lester, 2003). Bisphenol A is a chemical compound widely used as a raw material to manufacture chemical products such as polycarbonate plastics and epoxy resins. It is released into the environment during manufacturing processes and by leaching from final products (Staples *et al.*, 2000).

Numerous studies have reported the occurrence of BPA in the environmental matrices (Fromme *et al.*, 2002; Céspedes *et al.*, 2005) and in waste water treatment effluent because it is not completely removed during conventional treatments (Oulton *et al.*, 2010; Rodil *et al.*, 2012). Hence, to reduce its ubiquity in environmental matrices, it is necessary to develop sustainable treatment technologies to tackle this issue.

Advanced oxidation processes (AOPs) have proved to be a good alternative for the removal of recalcitrant compounds and the most popular AOPs studied are heterogeneous photocatalysis with semiconductors, ozonation and the photo-Fenton process (Klavarioti *et al.*, 2009). Heterogeneous photocatalysis and the photo-Fenton process are of special interest since sunlight can be used as the irradiation source (Malato *et al.*, 2009) while among the catalysts used in heterogeneous photocatalysis, TiO_2 has been gaining attention for its strong photoinduced oxidation power (Kaneco and Okura, 2002).

However, one disadvantage of TiO_2 is that it can only absorb UV light and this makes up only 3-5 % of solar light. Hence, many studies have been done to extend its photoactivity from UV into the visible light range in order to enable practical applications using solar energy (Byrne *et al.*, 2011). The strategies most employed are doping TiO_2-based materials with transition metals and with non-metallic elements (Rehman *et al.*, 2009).

Alternatively, when TiO_2-based materials are not doped, the key to using solar light efficiently is to have a catalyst with a higher photocatalytic activity. Some studies have shown that catalysts of high efficiency can be synthesized and obtained when some parameters such as crystal phases, particle size, surface area, particle morphology, distribution of hydroxyl groups, and charge separation are taken into

account and optimized (Ambrus *et al*., 2008; Fujishima *et al*., 2008). Increasing the surface area and charge separation can be achieved by anchoring TiO_2 particles onto substrates with a large surface area, such as mesoporous structures, zeolites or carbon-based materials where the graphene based composites look very promising. The combination of TiO_2 and graphene oxide could enhance the photodegradation of organic contaminants due to an improvement in electron transport, which prevents the recombination of charge, and to the adsorption capacity of organic contaminants on graphene oxide-TiO_2 (Nguyen-Phan *et al*., 2011).

In this context, innovative nanostructured UV-visible photocatalysts were synthesized within the collaborative project Clean Water FP7. These catalysts were tested for the degradation of several micropollutants. Previous results are presented elsewhere (Arana *et al*., 2010; Kontos *et al*., 2008; Pastrana-Martínez *et al*., 2012a, Pastrana-Martínez *et al*., 2012b). The objective of the present work is to evaluate the photocatalytic activity of the catalysts, synthesized during the Clean Water project, toward the degradation of an endocrine disruptor compound, bisphenol A, under both the UV part and the full spectrum of a simulated solar light. In this study, the photocatalytic activity of the catalysts is described not only with parameters like kinetic constant, conversion and mineralization percentages but also in terms of reactionnel intermediates and potential endocrine disruption effect of the treated solution.

In literature, the estrogenic effect of BPA intermediates is often measured using the Yeast Estrogen Screen (Chiang *et al*., 2004; Neamtu and Frimmel, 2006; Frontistis *et al*., 2011). This test, done *in vitro,* is able to detect estrogen agonists. However, the endocrine disruptor compounds do not only act as agonists of estrogen, they may also inhibit enzymatic catalysis reactions. In this case, only *in vivo* analysis could provide

a full spectrum of the disruption caused by these compounds in organisms. Thus, to identify a broad range of endocrine disruptor compounds, it is better to carry out estrogenic tests *in vivo* which enable the detection of estrogen agonists and antagonists, aromatizable androgens, activators and inhibitors of enzymatic catalysis reactions. In our study, to assess the estrogenic effect of intermediates formed during the photocatalytic degradation of BPA, a ChgH-GFP transgenic medaka line, was used. To our knowledge, this is the first study using this kind of test to detect the estrogenic effect of intermediates formed during an advanced oxidation process.

2. Materials and methods

2.1 Materials

Bisphenol A (BPA), hydroxyacetophenone and isopropylphenol were purchased from Sigma Aldrich. Titanium dioxide (AEROXIDE® TiO_2 P25, S_{BET} = 50 m^2/g) was obtained from Evonik Degussa GmbH (Frankfurt, Germany). Analytic reagents were obtained from Merck. Tree catalysts in powder form have been received from project partners: Non-doped TiO_2 (ECT-1023t, S_{BET} = 18.3 m^2/g), nitrogen-doped TiO_2 (N-TiO_2, S_{BET} = 141 m^2/g) and graphene oxide TiO_2 (GO-TiO_2, S_{BET} = 110 m^2/g). ECT-1023t was synthesized by means of a sol-gel method in which aggregates have been selected before thermal treatment (Arana *et al*., 2010); N-TiO_2 was synthesized as the hydrolysis condensation product of tetrabutyl titanate reaction with urea (Kontos *et al*., 2008) and GO-TiO_2 (graphene oxide content of 4.0 wt. %)

was prepared by liquid phase deposition followed by post-thermal reduction at 200 ºC (Pastrana-Martínez *et al*., 2012a).

2.2 Photocatalytic experiment

Photocatalytic experiments were carried out in a cylindrical reactor irradiated on the top with a solar simulator (Newport, USA), equipped with a Xenon arc lamp of 450 W (Figure 1). A quartz cover was placed on top of the glass reactor to minimize water loss due to evaporation. At the beam output, an AM 1.5 filter was placed to obtain a solar-like spectrum and, by using dichroic mirrors, a proper working wavelength range was selected. To conduct experiments, two wavelength ranges were chosen: 280-400 nm (UV) and 200 nm-30 μm (UV-visible). The intensity of light in different conditions (UV or UV-visible) was measured using a RAMSES-ARC-Hyperspectral UV-VIS Radiance Sensor-320-950 nm and a radiometer VLX-3W.The volume of the reactor was 1 L. Catalyst load (P25, ECT-1023t, N-TiO_2 and GO-TiO_2) and initial BPA concentration was 40 mg/L and 2 mg/L, respectively. During irradiation, the solution was shaken and continuously bubbled with air (~ 20 % of O_2) in order to maintain the solution in excess of O_2. Aliquots were taken every ten minutes to determine the BPA residual concentration, the dissolved organic carbon concentration and the endocrine disruption effect.

2.3 Analytical methods

The analysis of BPA and the degradation by-products was performed by HPLC (Model 600E, Waters) using a Nova Pack C18 reverse phase column (150 mm

141 × 3.9 mm, I.D. 4 µm, Waters). A mobile phase isocratic elution program was applied
142 with two solvents; Milli Q water and acetonitrile ($V_{water}/V_{acetonitrile}$ = 55/45) at a flow
143 rate of 1 mL/min. The detection was performed with a UV detector (Model 486,
144 Waters) at 226 nm. Dissolved Organic Carbon (DOC) was monitored with a
145 Shimadzu 5000 TOC analyzer. The detection and quantification limits were 70 µg/L
146 and 200 µg/L for the HPLC/UV and 16 µg/L and 32 µg/L for the TOC analyzer,
147 respectively.

148

149 **2.4 Evaluation of the endocrine disruption effect**

150 The estrogenic test was performed by the WatchFrog Company using a ChgH-
151 GFP transgenic medaka alevin line (international patent PCTWO 03/102176).
152 Transgenic medaka contain a green fluorescence protein (GFP) gene regulated by the
153 regulatory sequence of the choriogenin H (ChgH) gene. In this genetically modified
154 organism, estrogenic activity is indicated by fluorescence when exposed to estrogenic
155 compounds.

156 In a typical experiment, the estrogenic test is conducted in parallel in five vials and
157 repeated four times. The exposure time in each vial is 48 h at 26 °C. After 24 h, the
158 medium is renewed and finally, after 48 h, the fluorescence of alevin is observed with
159 a fluorescence microscope and quantified with Image J Software.

160 The test in each vial has a specific objective. The first three vials are used as control
161 test. In the fourth vial, alevins are exposed to 8 mL of sample taken during irradiation;
162 here estrogenic activator and inhibitor could be detected. In the fifth vial, alevins are
163 exposed to 8 mL of treated sample mixed with testosterone (30 µg/L). The addition of

testosterone enables the detection of the disturbance in the production of estradiol by aromataze enzyme to be detected. The aromataze enzyme ensures the equilibrium between estrogen and testosterone. So, in the fifth medium, activators and inhibitors of enzymatic catalysis reaction could be detected. More details on the test sample runs are given in Table I.

The results obtained on alevin fluorescence were analyzed according to the Organization for Economic Co-operation and Development (OECD) guidelines for the statistical analysis of ecotoxicity experiments (Document on the Statistical Analysis of Ecotoxicity Data, OCDE 2003) and were then classified into three levels of risk: 0, 1 and 2. In level 0, the fluorescence of alevin exposed to sample is not significantly different from alevin fluorescence in pure water; compounds in this sample are considered to be inert. In level 1, either the fluorescence of alevin exposed to treated sample differs significantly from that obtained in the negative control 1 so the compounds are suspected of having estrogenic effects, or the fluorescence of alevin exposed to sample with testosterone differs significantly from that obtained in the positive control 2 so the compounds are suspected of having effects on aromataze enzyme activity. In level 2, the fluorescence of alevin exposed to treated sample differs significantly from that obtained in the negative control 1 and the fluorescence of alevin exposed to sample with testosterone differs significantly from that obtained in the positive control 2; this sample contains compounds which present an estrogenic disruptor effect.

3. Results and discussion

3.1. Photocatalytic degradation

The photocatalytic degradation of BPA under the UV of the simulated solar light (280-400 nm) and under the full spectrum (UV-visible) of the simulated solar light (200 nm-30 µm) was carried out. The commercial catalyst P25 (AEROXIDE® TiO_2 Evonik Degussa) was used as a reference to compare the activity of the partner catalysts. The results obtained after 100 min of photocatalytic test are presented in Figure 2.

It can be observed that the photocatalytic degradation of BPA depends on the nature of the catalyst and the kind of the light irradiation (UV or UV-visible). After 100 min of photocatalysis under UV irradiation, P25 and ECT-1023t degraded BPA by 99 % and 76 %, respectively. GO-TiO_2 and N-TiO_2 were the less efficient catalysts; after 100 min only 40 % and 28 % of BPA was degraded, respectively. Under simulated UV-visible solar light and for the same irradiation time, 68, 54, 20 and 12 % of BPA is degraded using P25, ECT-1023t, N-TiO_2 and GO-TiO_2 respectively.

Measurement of the light intensity showed a decrease in the UV part of the simulated UV-visible solar irradiation. At 365 nm, the intensity was 2.35 mW/cm^2 under simulated UV light and 1.85 mW/cm^2 under simulated UV-visible light. This decrease in intensity may be the principal cause of the decrease in catalytic efficiency between irradiation under simulated UV solar light and simulated UV-visible solar light.

The activity of the synthesized photocatalysts was compared to P25. The main observations and the main results for each catalyst are listed below.

For ECT-1023t catalyst, the BPA conversion % and the apparent kinetic constant were higher than those of other partner catalysts but lower than those of P25. ECT-1023t catalyst has already been used to degrade phenolic compounds (phenol, catechol resorcinol, hydroquinone, *o*-aminephenol, *m*-aminephenol, *p*-aminephenol, *o*-cresol, *m*-cresol and *p*-cresol) and one pharmaceutical product (diphenhydramine). Its efficiency for phenolic compound degradation was higher than that of P25; the degradation rates were 2.7 times higher than those of Degussa P-25 (Arana *et al.*, 2008). The efficiency for diphenhydramine degradation depended on the catalyst loading; for an initial concentration of 100 mg/L of diphenydramine, ECT-1023t was more efficient than P25 for catalyst loadings higher than 1 g/L (Pastrana-Martínez *et al.*, 2012b). However, in this study, ECT-1023t efficiency for BPA degradation, for an initial BPA concentration of 2 mg/L and a catalyst concentration of 40 mg/L, was lower than for P25.

The photocatalytic activity of GO-TiO_2 has been also already evaluated for the degradation of organic compounds diphenhydramine (DP) and methyl orange (MO) and compared to that of P25 (Pastrana-Martínez *et al.*, 2012a). In the experimental condition used (DP/catalyst = 3.9×10^{-7} moles/mg, [MO]/[catalyst] = 6.1×10^{-8} moles/mg), GO-TiO_2 exhibited an higher photocatalytic activity than P25 for the degradation of these compounds. But in the present study GO-TiO_2 is less efficient than P25 for the degradation of bisphenol A. Taking into account the results obtained in aforementioned studies and in the present study, it could be said that the catalytic efficiency for the degradation of organic compounds depends on the substrate to be degraded and on the experimental conditions, for instance the catalyst loading.

For N-TiO_2, it can be noted that, in comparison with other catalysts, its efficiency is not so affected by the decrease in the intensity in the UV part of the UV-

visible simulated solar light. Under UV irradiation, 28 % of BPA was degraded while under the simulated solar light, 20 % of BPA was degraded. So, the catalyst N-TiO_2 is promising under visible light. This is in accordance with the results obtained by Kontos *et al*. (2008). During the synthesis of N-TiO_2, N was introduced at interstitial lattice sites. This induced a shift of the energy band gap to the visible range resulting in a significant visible light photocatalytic activity for N-TiO_2 (Kontos *et al*., 2008).

Since the disappearance of a compound does not mean that it was also mineralized, the DOC during the photocatalytic treatments was monitored. In Table II, values of the percentage of mineralization after 100 min are presented. Under UV irradiation, although BPA was 99 % removed, only 36 % of the initial DOC was removed with P25. A partial mineralization (10 %) was also obtained with ECT-1023t. With the other catalysts (N-TiO_2 and GO-TiO_2), BPA was not significantly mineralized after 100 min of irradiation. Under UV-visible irradiation, the same behavior was observed i.e. BPA was partially mineralized.

3.2. Monitoring of intermediates

The degradation of BPA and formation of intermediates were monitored by HPLC-UV. No intermediates were observed when N-TiO_2 and GO-TiO_2 catalysts were tested.

In Table III, the intermediates formed during the photocatalytic treatment under UV irradiation and UV-visible irradiation of the simulated solar light with P25 and ECT-1023t as catalysts are presented. These intermediates are named products 1, 2, 3, 4, 5 and 6, according to their respective elution order during HPLC analysis.

With P25, four main by-products were observed during the photocatalytic degradation of BPA under UV irradiation. With ECT-1023t, three main by-products were detected under the same conditions. According to the retention time, it seems that except for the by-product 2, the by-products obtained with the two catalysts are the same.

Under UV-visible irradiation, two additional intermediates (5 and 6) were detected; by-product 6 was observed only with ECT-1023t and product 5 was observed only with P25 (Table III).

The evolution of these intermediates during photocatalysis is presented in Figures 3 and 4. It can be seen that, under the same irradiation conditions, the distribution and the nature of intermediates are not the same when using ECT-1023t or P25. These observations suggest that the photocatalytic degradation pathway of BPA could be different depending on the catalyst used (ECT-1023t or P25).

With the same two catalysts but under different irradiation conditions, there are some differences regarding the detected intermediates (product 5 for P25 and products 6 and 2 for ECT). There are two possible explanations: 1) the reactive species created are different depending on the irradiation type or 2) the kinetic reactions under the respective irradiations are not the same. As under UV-visible irradiation the kinetics are lower than under UV irradiation, this observation strengthens the second assumption. This could then explain why, under UV-visible irradiation, more intermediates are detected. A further study must be done to identify the reactive species under UV and UV-visible irradiations with respect to the catalyst used in order to have more precise explanations.

3.4. Identification of intermediates

To determine the structure of the intermediate products formed during the photocatalytic treatment, the strategy was divided into 4 phases:

1) reviewing the literature,

2) listing the main BPA by-products often found in BPA photocatalysis,

3) analyzing the commercial by-products listed in 2) under the same conditions of BPA analysis, and finally,

4) comparing the retention times of commercial by-products with those of the intermediates formed during the treatment.

With the comparison of retention time, product 1 was identified as p-hydroxyacetophenone and product 6 as isopropylphenol. No match was found for the other by-products

p-hydroxyacetophenone is often found during BPA photocatalysis (Katsumata *et al.*, 2004; Li *et al.*, 2008; Inoue *et al.*, 2008). According to these authors, it could come from p-isopropenylphenol oxidation while p-isopropenylphenol could be formed after the loss of an H_2O molecule from 2-(4-hydroxyphenyl)-2-propanol or after a demethylation of p-isopropylphenol.

However, p-isopropylphenol (product 6) was not found in BPA photocatalysis when P25 was used (Table III). It was detected only with ECT-1023t as catalyst. From these observations, it can be supposed that, with P25 as catalyst, p-isopropenylphenol could be formed after the loss of an H_2O molecule from 2-(4-hydroxyphenyl)-2-propanol while with ECT-1023t as catalyst, p-isopropenylphenol could be formed by the same mechanism as well as after a demethylation of p-isopropylphenol (Figure 5). Further analysis by LC-MS/MS will be done in order to identify precisely these intermediates.

3.4. Endocrine disruption effect

During the photocatalytic treatment, BPA was partially mineralized and also transformed into other compounds. These intermediates were observed by HPLC-UV when P25 and ECT-1023t were used as catalysts. To test their potential toxicity, the estrogenic effect of the treated samples using these catalysts was evaluated. For both catalysts, the endocrine disruption effect of the treated solution was evaluated when the removal of BPA was estimated to be at approximately 50 % and to be higher than 90 %. Since the sampling times at which the toxicity tests have been realized are different depending on the catalyst. The estrogenic effect was evaluated after 20 min and 120 min of photocatalytic treatment using P25 and after 40 min and 140 min of photocatalytic treatment using ECT-1203t. Data showing the percentage of conversion and mineralization of BPA in these samples are given in Table IV. The samples were treated under UV of the simulated solar light (280-400 nm).

In Figures 6 and 7, the fluorescence of alevins after 48 h is presented. As can be observed, the initial solution of BPA (2 mg/L, t = 0 min) induced an alevin fluorescence higher than that in pure water and in the positive control 2 (alevin exposed to testosterone); BPA has an estrogenic effect and an effect on aromataze enzyme activity. The risk level is 2, confirming that BPA is an estrogenic disruptor compound.

With ECT-1023t catalyst (Figure 5), the sample taken after 40 min of photocatalytic treatment induced an alevin fluorescence higher than the negative control and, when the sample was mixed with testosterone, the alevin fluorescence was also higher than the positive control 2. The risk level is 2 so it could be concluded that, in this sample,

there are estrogenic disruptor compounds. The remaining BPA concentration after 40 min of photocatalysis was 900 µg/L. Thus, the estrogenic effect could be attributed to BPA remaining in the treated solution. After 140 min of photocatalytic treatment, alevin exposed to the sample fluoresced at the same magnitude as the negative control. After exposing alevin to the sample mixed with testosterone, fluorescence intensity was not statistically significant ($0.05 \leq p$) so it is considered to be the same as the positive control 2. Thus, the risk level is 0, the sample does not present an estrogenic effect and is considered as inert. After 140 min of photocatalysis with ECT-1023t, BPA was 90 % removed ([BPA] ≈ 200 µg/L) and around 18 % mineralized. It was transformed into other compounds which, according to the risk level result, are not considered estrogenic disruptors like BPA.

When the catalyst was P25 (Figure 7), the sample taken at 20 min also induced an alevin fluorescence higher than the negative control and, when mixed with testosterone, higher than the positive control 2. Since the remaining BPA concentration was 1300 µg/L, the estrogenic effect could also be attributed to BPA remaining in the solution. After 120 min of treatment, BPA was 99 % removed ([BPA] < DL) and 40 % mineralized. Alevin exposed to sample taken at this time (120 min) fluoresced at the same magnitude as the negative control but, in co-exposure with testosterone, the alevin fluorescence was higher than the positive control 2. Compounds in the sample after 120 min of photocatalysis act on aromataze activity and are suspected as being estrogenic disruptors.

A summary of the results from the estrogenic tests is given in Table V. Under UV irradiation, photocatalysis with ECT-1023t does not generate intermediates with an estrogenic effect. However, the photocatalytic treatment with P25 forms intermediates which are suspected as having an estrogenic effect. The monitoring of intermediates

354 with ECT and P25 showed that product 2 was formed only when the photocatalytic
355 experiment was performed with P25 (Table III), suggesting that this intermediate
356 could contribute to the detected estrogenic effect. Nevertheless, it must also be noted
357 that not all intermediates could be detected with HPLC/UV because of their low
358 concentration. Thus, other intermediates not observed could also be formed and these
359 could play a part in the estrogenic effect. Further work must be done to identify all the
360 intermediates.

361

362 **4. Conclusion**

363 The efficiency of ECT-1023t, N-TiO_2 and GO-TiO_2 in the degradation of BPA under
364 the UV part of a simulated solar light and under the UV-visible part of the same
365 simulated solar light was evaluated. These catalysts exhibited a significant
366 degradation of BPA and, among them, ECT-1023t was the most efficient in terms of
367 BPA conversion and mineralization. The intermediates obtained with P25 (reference)
368 and ECT-1023t as catalysts were monitored and some of them were identified. It
369 appears that the reaction intermediates found in solution depend on the catalyst type
370 and the kinetic reaction rate. Under the UV part of the simulated solar light, the by-
371 products generated when using ECT-1023t as catalyst do not present any estrogenic
372 effect like BPA does. Based on these observations, we can highlight that ECT-1023t
373 is a promising catalyst for the photocatalytic treatment of water under solar light

374 **Acknowledgment**

375 We are grateful for the funding of the European Commission through the Clean Water
376 Project which is a Collaborative Project (Grant Agreement number 227017) co-

377 funded by the Research DG of the European Commission within the joint RTD
378 activities of the Environment and NMP Thematic Priorities.

379

380 **References**

381 Ambrus, Z., Mogyorósi, K., Szalai, Á., Alapi, T., Demeter, K., Dombi, A., Sipos, P.
382 (2008) Low temperature synthesis, characterization and substrate-dependent
383 photocatalytic activity of nanocrystalline TiO_2 with tailor-made rutile to anatase ratio.
384 Applied Catalysis A: General 340 (2), 153-161.

385 Araña, J., Doña-Rodríguez, J. M., Portillo-Carrizo, D., Fernández-Rodríguez, C.,
386 Pérez-Peña, J., González Díaz, O., Navío, J. A., Macías, M. (2010) Photocatalytic
387 degradation of phenolic compounds with new TiO_2 catalysts. Applied Catalysis B:
388 Environmental 100 (1-2), 346-354.

389 Birkett, J. W., Lester, J. N. (2003) endocrine disrupters in wastewater and Sludge
390 Treatment Processes. IWA Publishing, Lewis Publishers, London, 295p.

391 Byrne, J. A., Fernandez-Ibañez, P. A., Dunlop, P. S. M., Alrousan, D. M. A.,
392 Hamilton, J. W. J. (2011) Photocatalytic Enhancement for Solar Disinfection of
393 Water: A Review. International Journal of Photoenergy, 2011.

394 Céspedes, R., Lacorte, S., Raldúa, D., Ginebreda, A., Barceló, D., Piña, B. (2005)
395 Distribution of endocrine disruptors in the Llobregat River basin (Catalonia, NE
396 Spain). Chemosphere 61(11), 1710-1719.

397 Chiang K., Lim T. M., Tsen L., Lee C. C. (2004) Photocatalytic degradation and
398 mineralization of bisphenol A by TiO_2 and platinized TiO_2. Applied Catalysis A, 261,
399 225-237.

400 Fromme, H., Küchler, T., Otto, T., Pilz, K., Müller, J., Wenzel, A. (2002) Occurrence
401 of phthalates and bisphenol A and F in the environment. Water Research 36 (6), 1429-
402 1438.

403 Frontistis, Z., Daskalaki, V. M., Katsaounis, A., Poulios, I., Mantzavinos, D. (2011)
404 Electrochemical enhancement of solar photocatalysis: Degradation of endocrine
405 disruptor bisphenol-A on Ti/ TiO_2 films. Water Research 45 (9), 2996-3004.

406 Fujishima, A., Zhang, X., Tryk, D. A. (2008) TiO_2 photocatalysis and related surface
407 phenomena. Surface Science Reports 63 (12), 515-582.

408 Inoue, M., Masuda, Y., Okada, F., Sakurai, A., Takahashi, I., Sakakibara, M. (2008)
409 Degradation of bisphenol A using sonochemical reactions. Water Research 42(6–7),
410 1379-1386.

411 Kaneko, M., Okura, I. (2002) Photocatalysis, 18-27, Springer, Tokyo.

412 Katsumata, H., Kawabe, S., Kaneco, S., Suzuki, T., Ohta, K. (2004) Degradation of
413 bisphenol A in water by the photo-Fenton reaction. Journal of Photochemistry and
414 Photobiology A. 162 (2–3), 297-305.

415 Klavarioti, M., Mantzavinos, D., Kassinos, D. (2009) Removal of residual
416 pharmaceuticals from aqueous systems by advanced oxidation processes.
417 Environment International 35 (2), 402-417.

418 Kontos, A. I., Kontos, A. G, Raptis, Y. S., Falaras, P. (2008) Nitrogen modified
419 nanostructured titania: electronic, structural and visible-light photocatalytic properties.
420 Physica Status Solidi, 2, 83-85.

421 Li, C., Li, X. Z., Graham, N., Gao, N. Y. (2008) The aqueous degradation of
422 bisphenol A and steroid estrogens by ferrate. Water Research 42(1–2), 109-120.

423 Malato, S., Fernández-Ibáñez, P., Maldonado, M. I., Blanco, J., Gernjak, W. (2009)
424 Decontamination and disinfection of water by solar photocatalysis: Recent overview
425 and trends. Catalysis Today 147 (1), 1-59.

426 Neamtu, M., Frimmel, F. H. (2006) Degradation of endocrine disrupting bisphenol A
427 by 254 nm irradiation in different water matrices and effect on yeast cells. Water
428 Research, 40, 3745–3750.

429 Nguyen-Phan, T., Pham, V. H., Shin, E. W., Pham, H., Kim, S., Chung, J. S., Kim, E.
430 J., Hur, S. H. (2011) The role of graphene oxide content on the adsorption-enhanced
431 photocatalysis of titanium dioxide/graphene oxide composites. Chemical Engineering
432 Journal, 170, 226-232.

433 Oulton, R. L., Kohn, T., Cwiertny, D. M. (2010) Pharmaceuticals and personal care
434 products in effluent matrices: A survey of transformation and removal during
435 wastewater treatment and implications for wastewater management. Journal of
436 Environmental Monitoring, 12, 1956-1978.

437 Pastrana-Martínez, L. M., Faria, J. L., Doña-Rodríguez, J. M., Fernández-Rodríguez,
438 C., Silva, A. M. T. (2012b) Degradation of diphenhydramine pharmaceutical in
439 aqueous solutions by using two highly active TiO_2 photocatalysts: Operating
440 parameters and photocatalytic mechanism. Applied Catalysis B: Environmental, 113–
441 114, 221-227.

442 Pastrana-Martínez, L. M., Morales-Torres, S., Likodimos, V., Figueiredo, J. L., Faria,
443 J. L., Falaras, P., Silva, A. M. T. (2012a) Advanced nanostructured photocatalysts

444 based on reduced graphene oxide-TiO_2 composites for degradation of
445 diphenhydramine pharmaceutical and methyl orange dye. Applied Catalysis B:
446 Environmental, 123-124, 241-256.

447 Rehman, S., Ullah, R., Butt, A. M., Gohar, N. D. (2009) Strategies of making TiO_2
448 and ZnO visible light active. Journal of Hazardous Materials 170 (2–3), 560-569.

449 Rodil, R., Quintana, J. B., Concha-Graña, E., López-Mahía, P., Muniategui-Lorenzo,
450 S., Prada-Rodríguez, D. (2012) Emerging pollutants in sewage, surface and drinking
451 water in Galicia (NW Spain). Chemosphere 86 (10), 1040-1049.

452 Staples, C. A., Dorn, P. B., Klecka, G. M., Oblock, S. T., Branson, D. R., Harris, L. R.
453 (2000) Bisphenol A concentrations in receiving waters near US manufacturing and
454 processing facilities. Chemosphere 40 (5), 521-525.

455 Staples, C. A., Dome, P. B., Klecka, G. M., Oblock, S. T., Harris, L. R. (1998) A
456 review of the environmental fate, effects, and exposures of bisphenol A. Chemosphere
457 36 (10), 2149-2173.

458

459

Highlights

"The ECT-1023t catalyst degrades bisphenol A efficiently under simulated solar light". "The catalyst N-TiO_2 is efficient under the visible part of the simulated solar light". "Formation of intermediates depends on the catalyst type". "Intermediates of the reaction with ECT-1023t as catalyst have no estrogenic effect".

Figure 1: Photocatalytic reactor

Figure 2: Percentage of conversion of BPA and apparent kinetic constants during photocatalytic treatment under (a) UV of simulated solar light (280-400 nm) and (b) under the full spectrum of simulated solar light (200 nm-30 µm)

Figure 3: Monitoring of BPA intermediates formed when using P25 (a) and ECT-1023t (b) under UV irradiation (280-400 nm).

Figure 4: Monitoring of BPA intermediates formed when using P25 (a) and ECT-1023t (b) under UV-visible irradiation (200 nm- 30 µm).

Figure 5: Proposed reaction mechanism for BPA degradation

Figure 6: Fluorescence of alevins exposed to (a) samples treated with ECT-1023t and (b) samples treated with ECT-1023t mixed with testosterone (NS: statistically not significant).

Figure 7: Fluorescence of alevins exposed to (a) samples treated with P25 and (b) samples treated with P25 mixed with testosterone (NS: statistically not significant).

Table I: Description of the samples in the estrogenic effect evaluation test.

Name of sample	**Contents**	**Objectives**
Negative control	Alevin, 8 mL of pure water	Gives the level of alevin fluorescence
Positive control 1	Alevin, 300 ng/L of EE2 in water	Gives the level of alevin fluorescence in contact with hormone with an estrogenic effect
Positive control 2	Alevin, 30 µg/L of testosterone in water	Gives the level of aromataze enzyme activity
Raw sample	Alevin, sample taken during the treatment	Indicates the estrogenic effect of the treated sample
Sample doped with testosterone	Alevin, sample taken during the treatment, testosterone 30 µg/L	Indicates the effect of treated sample on aromataze enzyme activity

EE2: Ethinylestradiol

Table II: Percentage of mineralization of BPA after 100 minutes of photocatalytic treatment.

	UV (280-400 nm)	UV-visible (280-30 µm)
N-TiO_2	≤ LD	≤ LD
ECT-1023t	10	4
P25	36	24
GO-TiO_2	4	≤ LD

Table III: Intermediates found during the photocatalytic degradation test.

	UV		**UV-visible**	
	P25	**ECT-1023t**	**P25**	**ECT-1023t**
Product 1 Rt = 1.7 min	×	×	×	×
Product 2 Rt = 1.9 min	×	None	×	×
Product 3 Rt = 2.3 min	×	×	×	×
Product 4 Rt = 2.7 min	×	×	×	×
Product 5 Rt = 3.2 min	None	None	×	None
Product 6 Rt = 4.6 min	None	None	None	×

Rt: retention time, ×: detected, none: not detected.

Table IV: Percentage of mineralization and BPA conversion in the samples tested to assess the estrogenic effect

	P25		**ECT-1023t**	
	20 min	**120 min**	**40 min**	**140 min**
% conversion	35	99	55	90
% mineralization	10	40	5	18

Table V: Evaluation of the endocrine disruption effect

	Time treatment (min)	**BPA % conversion**	**BPA % mineralization**	**Risk level in estrogenic test**	**Conclusion**
ECT-1023t	40	55	5	Level 2	Estrogenic disruptor
	140	90	18	Level 0	No effect
P25	20	35	10	Level 2	Estrogenic disruptor
	120	99	40	Level 1	Suspected

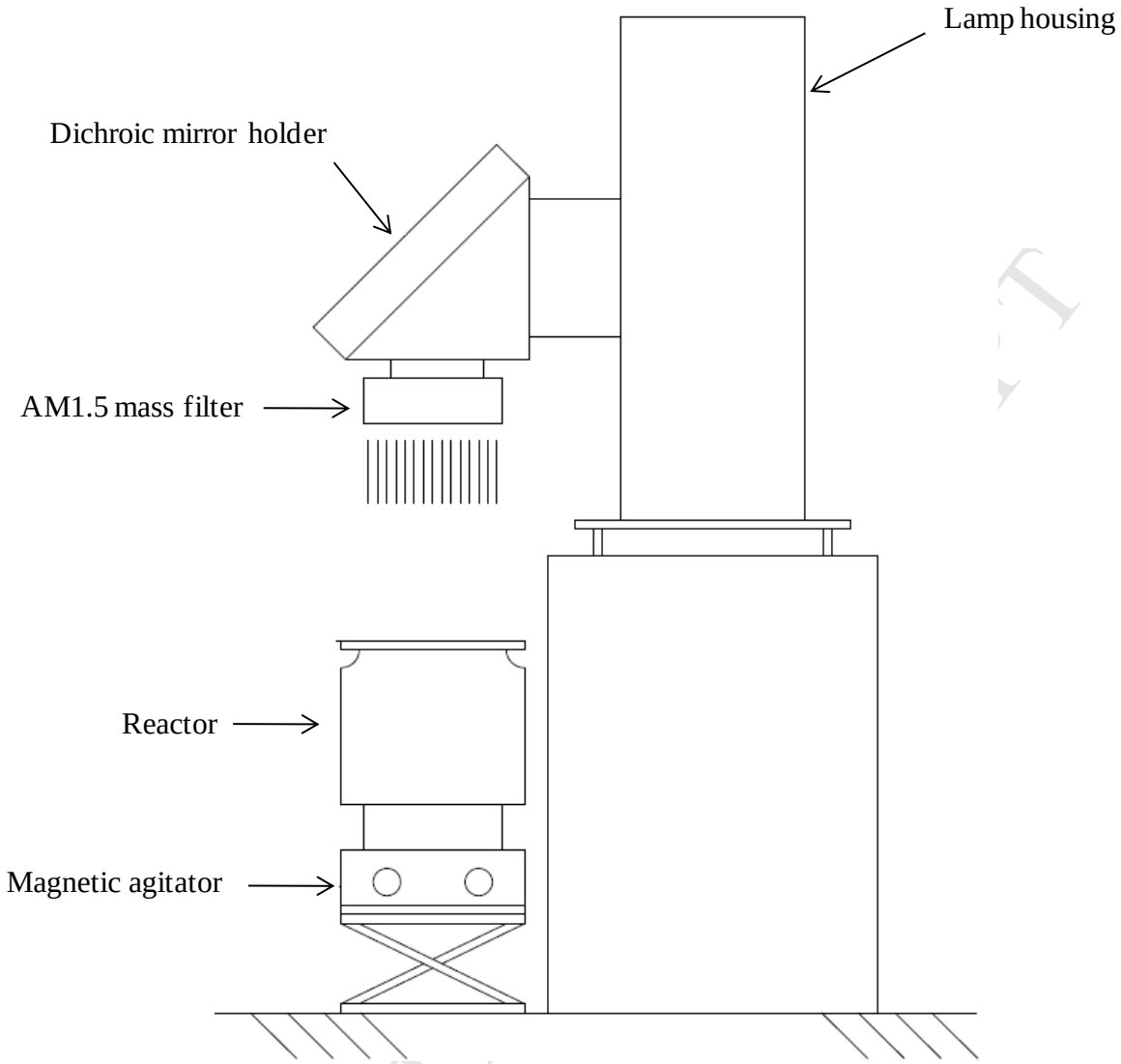

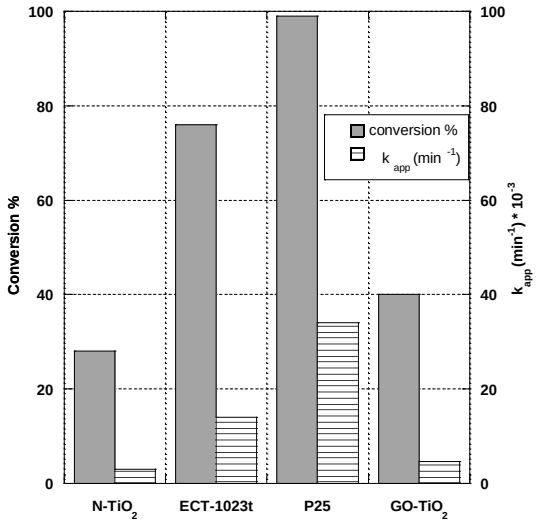

(a)

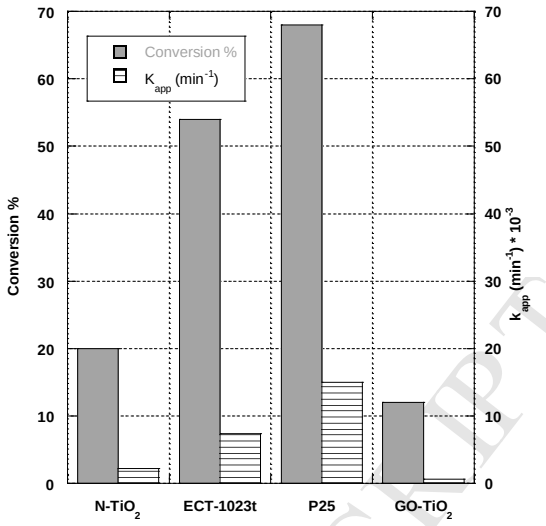

(b)

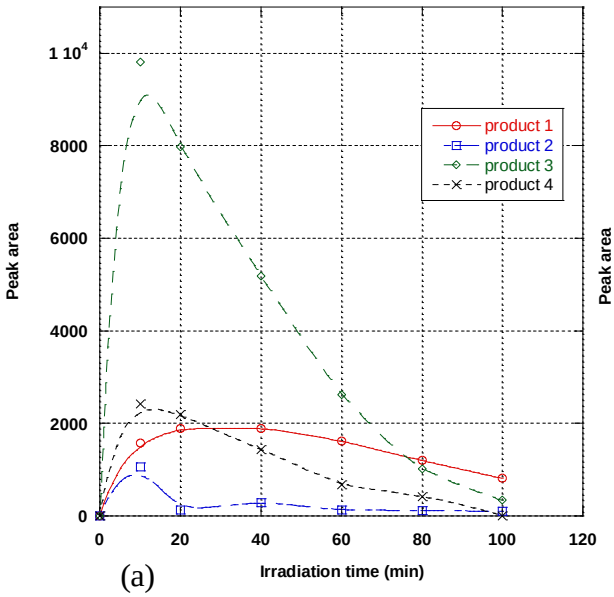

(a)

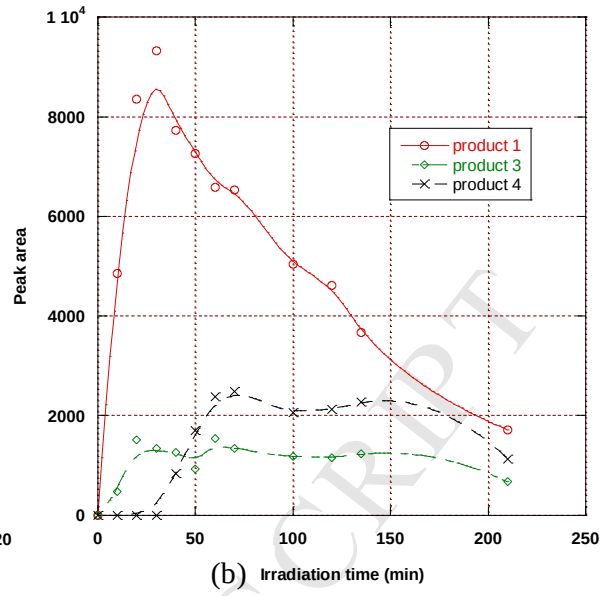

(b)

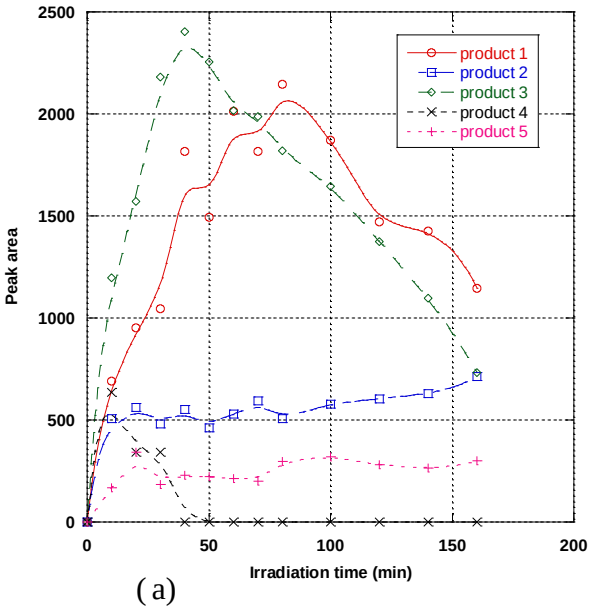

(a)

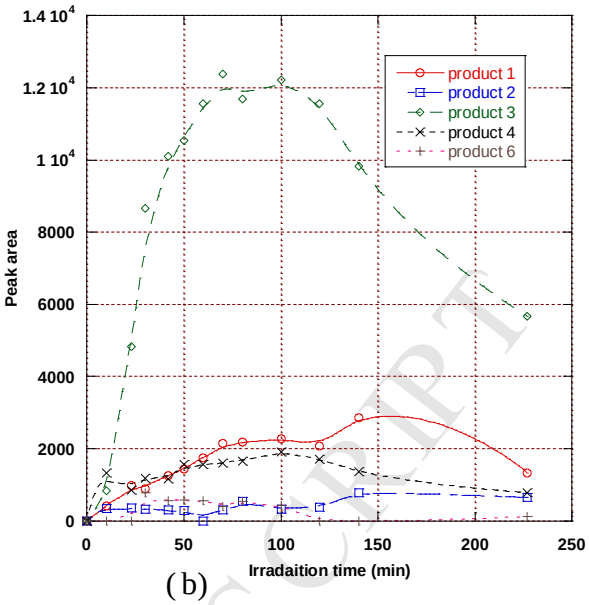

(b)

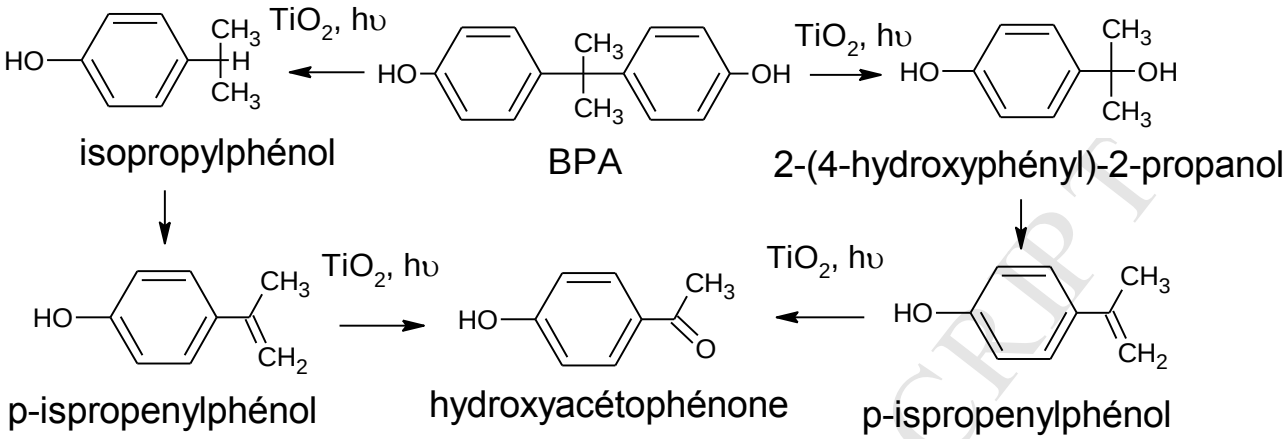

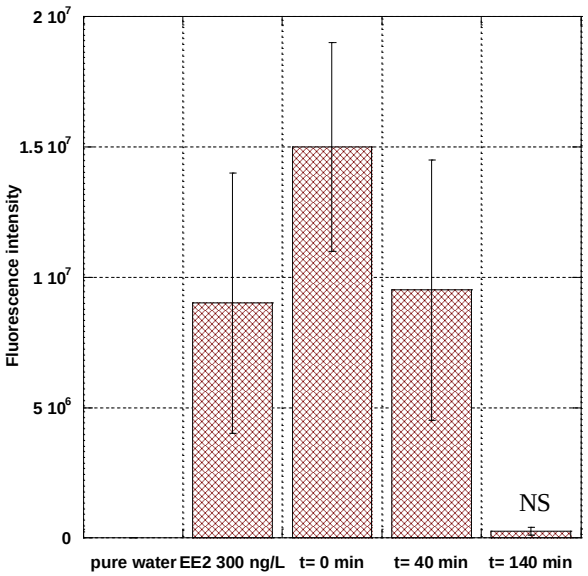

(a)

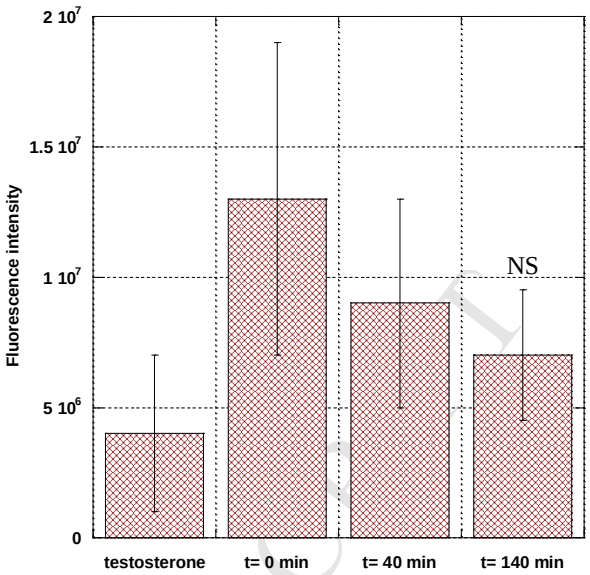

(b)

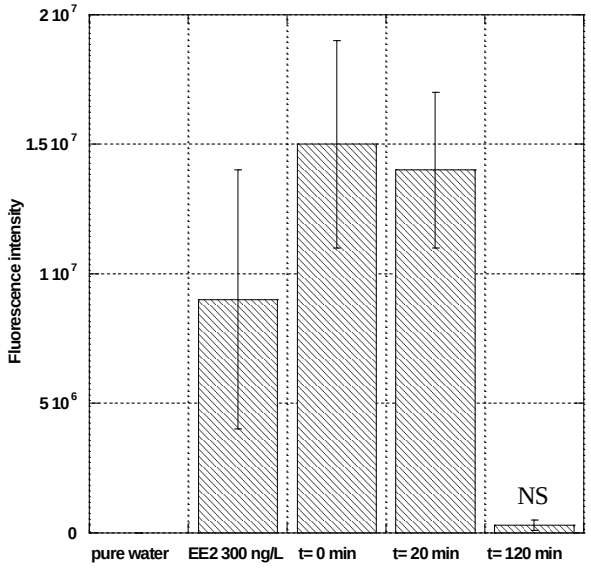

(a)

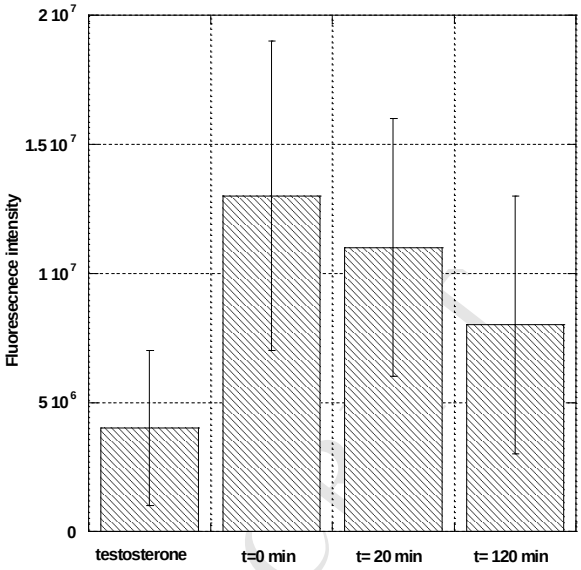

(b)